CONTRAST MEDIA & MOLECULAR IMAGING

Received: 13 August 2010, Revised: 16 December 2010, Accepted: 10 January 2011, Published online in Wiley Online Library: 2011

(wileyonlinelibrary.com) DOI: 10.1002/cmmi.436

MRI of cells and mice at 1 and 7 Tesla with Gd-targeting agents: when the low field is better!

Simonetta Geninatti-Crich[a], Ibolya Szabo[a], Diego Alberti[a], Dario Longo[a] and Silvio Aime[a]*

Tumor cells were targeted with Gd-loaded/LDL (low density lipoproteins) adducts consisting of *ca* 300 Gd(III) amphiphilic complexes incorporated in the lipophilic LDL particles. The long reorientational time of the Gd(III) complex in the supramolecular adduct yielded a relaxivity peak at *ca* 1 T, whereas its relaxivity at 7 T was 5 times less. The field-dependent relaxivity markedly affected the signal enhancement attainable at the two magnetic fields. As tumor cells showed up-regulation of LDL transporters, B16 melanoma cells were labeled with the Gd-loaded/LDL adduct. Each cell contained *ca* 2×10^9 Gd atoms. Upon dispersion of 5000 labeled cells in 1 μl of agar, signal intensity (SI) enhancements of about 30 and 7% were observed at 1 and 7 T, respectively. The results obtained on cellular systems were confirmed *in vivo* upon the administration of Gd-loaded/LDL particles to C57 mice bearing a transplanted melanoma (B16) tumor. From the herein reported results, one may conclude that, for slowly moving Gd complexes, it is possible to obtain *in vivo* sensitivity enhancements at 1 T several times higher than that attained at high fields. Copyright © 2011 John Wiley & Sons, Ltd.

Keywords: MRI; low field; LDL; Gd complexes; macromolecular imaging probes

1. INTRODUCTION

Contrast in magnetic resonance (MR) images arises mainly from differences in water proton relaxation time. The contrast can be enhanced using paramagnetic metal complexes, mainly Gd(III) complexes, that markedly increase the water proton relaxation rates in the regions where they distribute (1–4). The ability of a paramagnetic metal complex to act as a MRI contrast agent is related to its relaxivity (r_1), which is the relaxation enhancement of water protons at 1 mM concentration of the metal complex. The relaxivity of Gd(III) complexes is field-dependent and, in the case of the paramagnetic complex is part of a macromolecular system, it shows a maximum efficiency at *ca* 1 T (5,6). The theory of paramagnetic relaxation accounts well for this experimental observation as, at around 1 T, provided that the exchange rate of the metal coordinated water is fast, there is a dominant effect of the long reorientational motion of the paramagnetic macromolecule (7). Currently, most MRI scanners for small animals employ superconducting magnets that work at fields from 4.7 to 7 T (and even higher ones). High fields provide an overall increase of the signal intensity (SI) that allows the rapid acquisition of highly resolved images. However, in the presence of macromolecular Gd(III) contrast agents, the benefit on SI brought by the relaxation enhancement observed at low fields may well counterbalance the advantages offered by the high fields. This work aims at comparing *in vitro* and *in vivo* results obtained at 1 and 7 T using as Gd(III) targeting agent the supramolecular adduct formed by amphiphilic Gd(III) complexes (Gd–AAZTAC17; Fig. 1) incorporated into low density lipoprotein (LDL) particles. The used amphiphilic Gd(III) complex corresponds to the Gd–AAZTA complex in which the exocyclic carbon has been replaced by a long -C_{17} alkyl chain in order to pursue the incorporation in the lipidic core of LDL particles (8,9). To carry out the proposed comparison a newly available 1 T scanner by Aspect (Aspect Magnet Technologies Ltd, Netanya, Israel) based on a NdFeB permanent magnet was used. This scanner displays an excellent in plane spatial resolution (less than 100 μm) that is a prerequisite in order to acquire images of small animals like mice.

2. RESULTS AND DISCUSSION

Gd-loaded/LDL particles, used as imaging probes, were prepared following the already reported procedure. (9) Each LDL particle can be loaded with 250–300 Gd–AAZTAC17 molecules. The LDL particles are formed by a high molecular weight protein (*ca* 500 kDa) that wraps around a lipidic core incorporating the aliphatic chain of the amphiphilic Gd(III) complex. No significant change was observed in the size of the LDL particles (22 ± 1 nm diameter) upon loading with Gd–AAZTAC17 molecules. Since in aqueous solutions Gd–AAZTAC17 self-assembles into 7 nm micelles that exhibit a critical micelle concentration (cmc) of 0.1 mM (8), the LDL loading protocol was carried out using Gd complex concentrations lower than the cmc (0.08 mM). Under these conditions, the Gd complex interacts with the protein in its monomeric form, thus avoiding a radical change in the native protein structure. The binding affinity of Gd–AAZTAC17 with LDL

* *Correspondence to: S. Aime, Department of Chemistry I.F.M, and Center for Molecular Imaging, University of Torino, Torino, Italy. E-mail: silvio.aime@unito.it*

a *S. Geninatti-Crich, I. Szabo, D. Alberti, D. Longo, S. Aime Department of Chemistry I.F.M, and Center for Molecular Imaging, University of Torino, Torino, Italy*

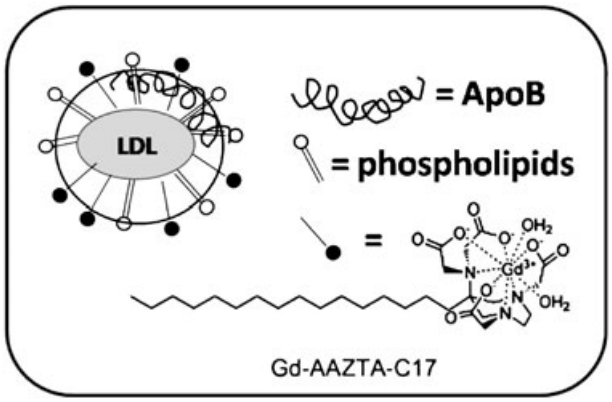

Figure 1. Schematic representation of LDL labeled with Gd–AAZTAC17 complex.

is very high ($K_a = 1 \times 10^5$ M^{-1}) (9) and the amount of dissociated Gd–AAZTAC17 from the supramolecular adduct does not reach the cmc for the micelle formation. Gd–AAZTAC17/LDL adduct displays a high relaxivity ($r_{1p} = 20.4$ mM^{-1} s^{-1}) at 1 T (40 MHz) as witnessed by recording the $1/T_1$ NMRD profile (Fig. 2). Conversely, the relaxivity at 7 T (300 MHz) is five times lower ($r_{1p} = 4.0$ mM^{-1} s^{-1}).

The relaxivity behavior is fully consistent with the established theory of paramagnetic relaxation for slowly moving macro- and supra-molecular systems. On the basis of the observed T_1 values, it is possible to calculate, using equation (1), the SI enhancement that should be obtained in the corresponding spin-echo T_1-weighted images acquired at 1 and 7 T, respectively.

$$SI = K \times \rho \times \{1 - \exp[-(TR - TE)/T_1)] \times \exp(-TE/T_2)\} \quad (1)$$

where K represents the influence of flow, perfusion, and diffusion; ρ is the proton density; TR is the repetition time; TE is the echo time; and T_1 and T_2 are the longitudinal and transverse water proton relaxation times, respectively.

Since, in molecular imaging applications the concentrations of Gd-based imaging probes at the target sites are usually <100 μM, %SI enhancements have been calculated using equation (1) as a function of TR at 1 and 7 Tesla, assuming Gd–AAZTAC17/LDL solutions with concentrations of 100 and 50 μM (Fig. 3). As expected, %SI enhancements of Gd–AAZTAC17/LDL containing solutions are inversely proportional to TR at both fields. Furthermore, the difference of the SI enhancement measured at 1 T with respect to that measured at 7 T increases when TR decreases. When using a TR of 250 ms, an increase of more than three times is expected at 1 T with respect to 7 T using these macromolecular LDL-based systems. Therefore, a TR of 250 ms has been used in both *in vivo* and *in vitro* MRI experiments carried out in this study.

Next, the 1–7 T comparison was carried out on a tumor cell line (mouse melanoma B16–F10) and in the corresponding xenografted mouse model. LDL particles are avidly taken up by tumor cells that need their lipidic payload to form cellular and organelle membranes in their proliferative process. LDLs accumulate in cells through an upregulation of their transporters (10–12). The uptake process leads to the internalization of LDL particles into endosomes where they are de-assembled by the action of the acidic pH and of specific enzymes (13,14). As far as the intracellular enhancement properties of the MR imaging reporter are concerned, one can foresee that, also upon the occurrence of endosomal LDL de-assembling process, Gd–AAZTAC17 would maintain an analogous relaxation behavior if it either aggregates to form micelles or is incorporated into any phospholipid membrane. In both cases the amphiphilic Gd–AAZTAC17 complex will be characterized by a reduced mobility and the observed relaxivity will be essentially determined by the exchange rate of the coordinated water. B16 melanoma was labeled by incubating cells in the presence of Gd–AAZTAC17/LDL adduct (60 μg ml^{-1}) for 12 h. After several washings, cells underwent MRI scrutiny. To this purpose, a phantom formed by four capillaries, each containing cells dispersed in agar, was prepared. One capillary contained unlabeled B16 cells (control) whereas the remaining three contained 20 000, 10 000 and 5000 labeled cells μl^{-1}, respectively. Images were acquired at 1 and 7 T, and the results are shown in Fig. 4(A).

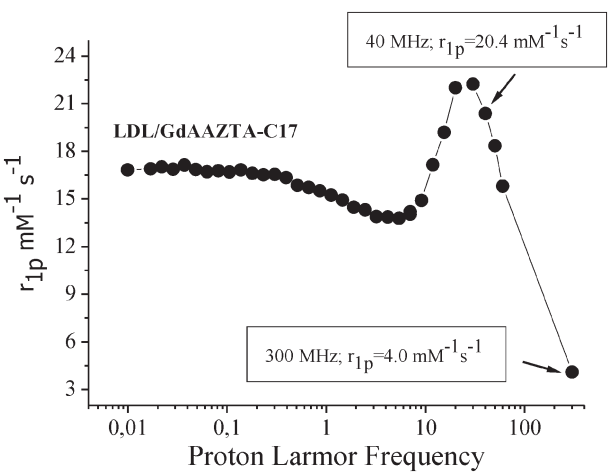

Figure 2. $1/T_1$ ^{1}H NMRD profile (0.01–80 MHz, pH 7, and 25 °C) of Gd–AAZTAC17/LDL (250:1) adduct. The profile was acquired using 0.08 mM Gd complex solution and normalized to the relaxivity (mM^{-1} s^{-1}).

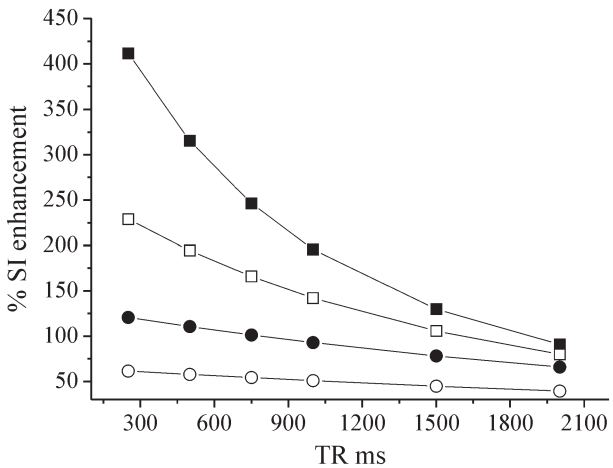

Figure 3. Percentage SI enhancements of 100 (solid symbols) and 50 μM (open symbols) Gd–AAZTAC17/LDL solutions calculated as a function of TR using equation (1). Squares and circles correspond to 1 and 7 T field strengths, respectively. Relaxivities of 20.4 and 4.0 mM^{-1} s^{-1} have been used in the calculations at 1 and 7 T, respectively.

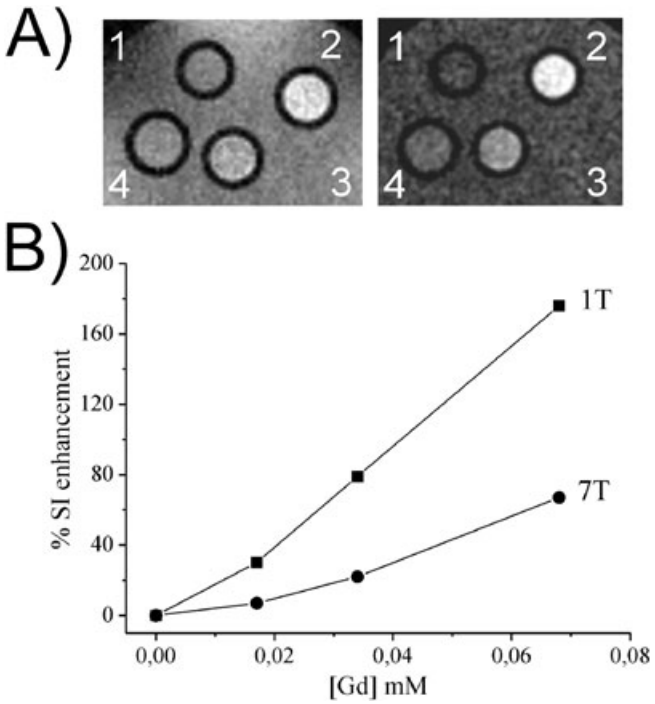

Figure 4. (A) T_1-weighted spin echo image, recorded at 1 and 7 T, of an agar phantom containing B16 cells labeled with Gd–AAZTAC17/LDL adduct. Cells are dispersed in agar at different densities: (1) control unlabeled cells; (2) 20 000 cells μl^{-1}; (3) 10 000 cells μl^{-1}; (4) 5000 cells μl^{-1}. (B) %SI enhancement, measured at 1 and 7 T, as a function of Gd intracellular concentration determined on labeled cells by ICP-MS. Gd concentrations of 0.068, 0.034 and 0.017 mM correspond to 20 000, 10 000 and 5000 cells μl^{-1}, respectively.

Clearly, the SI enhancements of labeled cells measured at 1 T were markedly higher than those measured at 7 T at all three investigated concentrations. The amount of Gd internalized by cells, as measured by ICP-MS, was 3.4×10^{-9} μmol Gd per cell. Percentage SI enhancements and corresponding T_1 measured on cell-containing capillaries were compared with those calculated on the basis of Gd concentrations in agar capillaries (Table 1).

The measured values were lower than the corresponding calculated values. The reason for such mismatch relies on the fact that the 'apparent' Gd millimolar relaxivities (r_{1p}) of internalized Gd–AAZTAC17 were only 14.6 and 3.6 mM^{-1} s^{-1}at 1 and 7 T, respectively. These values were significantly lower than the values measured at the same magnetic field strength in the aqueous solution reported above. This observation supports the view that the Gd–AAZTAC17/LDL is internalized through receptor-mediated endocytosis. As previously shown (15–17), the occurrence of a lower r_{1p} value is a good indication that the Gd complexes are confined in endosomal vesicles, resulting in a 'quenching' of the observed relaxivity. The endosomal localization of the imaging probe was confirmed by confocal analysis using rhodamine labeled Gd–AAZTAC17/LDL (9). Figure 4(B) shows the direct comparison between %SI enhancement measured at 1 and 7 T. Any Gd concentration value measured at 1 T yielded significantly higher %SI than at 7 T. In particular, the capillary containing 5000 cells μl^{-1} was not significantly different from the control at 7 T, whereas at 1 T it still showed a 30% enhancement over the control. Thus, at 1 T, the detection threshold appeared for Gd-labeled cells well below 5000 cells μl^{-1}. These *in vitro* results clearly anticipate the advantages of using targeted macromolecular Gd(III)-based probes for *in vivo* application at low fields (1 T).

Next, the comparison was carried out on mouse models bearing a tumor xenograft obtained by subcutaneous injection of *ca* 1 million B16 cells. After 7 days, the tumor volume was between 30 and 60 mm^3. Gd–AAZTAC17/LDL adducts were administered intravenously at a 0.06 mmol kg^{-1} Gd dose. An external reference tube (5 mm diameter) containing a GdHPDO3A solution, 0.5 mM, was used to quantify the %SI enhancement in the images acquired at 1 and 7 T, respectively. Images were recorded 5 h after the i.v. administration of the Gd–AAZTAC17/LDL adduct solution. All mice ($n = 3$) were imaged PRE and POST contrast injection on both scanners. Mice were first imaged at 7 T (acquisition time *ca* 15 min) and then at 1 T (acquisition time *ca* 30 min). Gd-loaded LDL particles were administered to mice immediately after the acquisition of PRE contrast images. POST contrast images were acquired, in the same order, 5 h after the administration of the contrast agent. As shown in Fig. 5, tumor cells took up the paramagnetic LDL particles and the resulting contrast wass markedly higher in the T_1-weighted SE image acquired at 1 T with respect to 7 T. Quantitatively, the measured %SI enhancement of the tumor region at the two fields resulted was 80 ± 9 and 30 ± 13%, respectively (using a *TR* of 250 ms). Using different number of scans (see the Experimental), similar SNRs (signal-to-noise ratio) of 24 ± 4 and 22 ± 2 were obtained at 7 and 1 T, respectively. Since the T_1 values of adjacent tissues were shorter at low field, contrast-to-noise ratios (CNR) were calculated in order to evaluate the capability of the imaging probe to discern the target tissue. At 1 T, CNR was 10 ± 3, i.e. a value that is more than the twice of that measured at 7 T (4 ± 1.5).

Table 1. Comparison between %SI and R_1 measured on cells dispersed in agar with respect to the corresponding calculated values on the basis of equation (1) using the Gd concentrations obtained from ICP-MS measurements (0.068, 0.034 and 0.017 mM for 20 000, 10 000 and 5000 cells μl^{-1}, respectively)

Cells μl^{-1}	Measured %SI (1 T)	Expected %SI (1 T)	Measured R_1 s^{-1} (1 T)	Expected R_1 s^{-1} (1 T)	Measured %SI (7 T)	Expected %SI (7 T)	Measured R_1 s^{-1} (7 T)	Expected $R_1 s^{-1}$ (7 T)
20 000	176	293	1.34	1.69	67	82	0.546	0.571
10 000	79	130	0.752	0.990	22	41	0.400	0.435
5000	30	61	0.526	0.667	7	21	0.340	0.370
Ctrl	0	0	0.366	0.366	0	0	0.303	0.303

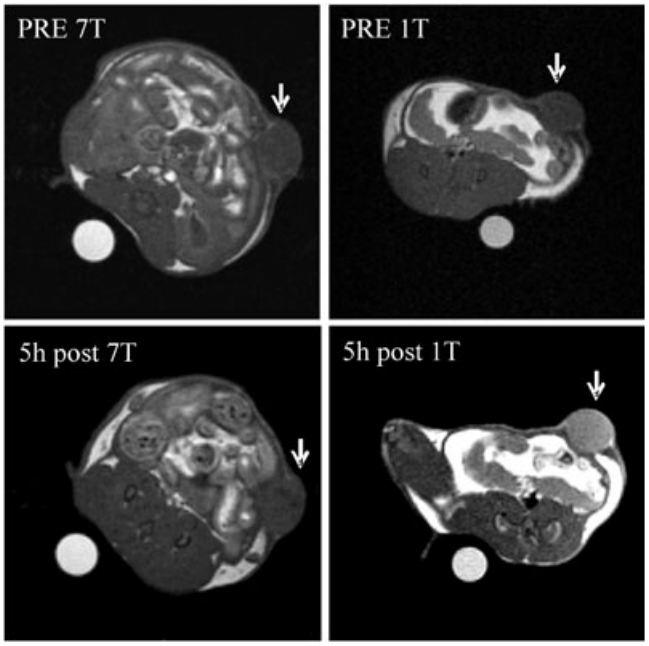

Figure 5. T_1-weighted multislice spin echo MR images of C57BL/6 mice grafted subcutaneously with B16 melanoma cells. Images were obtained before (PRE) and 5 h after the administration of Gd–AAZTAC17/LDL 0.06 mmol kg^{-1}. Arrows show the enhanced tumor region (outlined in blank). Percentage SI enhancement of tumor region at the two fields was 80 ± 9 and 30 ± 13% at 1 and 7 T, respectively.

3. CONCLUSIONS

The reported results indicate that, for applications in which the paramagnetic agent is bound to a macromolecular system in slow-moving conditions, a high-resolution 1 T scanner is preferable to a high-field one. Many molecular imaging applications can be properly carried out at this (low) field when using Gd(III)-based probes possessing long molecular correlation time and functionalized with targeting moiety. The availability of low-cost, easy-to-use 1 T MRI scanners may markedly increase the number of biological groups that should come to consider *in vivo* MRI as a complementary or alternative tool to other imaging modalities.

4. EXPERIMENTAL

The $1/T_1$ nuclear magnetic relaxation dispersion profiles of water protons were measured over a continuum of magnetic field strength from 0.00024 to 0.5 T (corresponding to 0.01–20 MHz proton Larmor frequency) on the fast field-cycling Stelar Spinmaster FFC 2000 relaxometer equipped with a silver magnet. The relaxometer operated under complete computer control with an absolute uncertainty in the $1/T_1$ values of ±1%. The typical field sequences used were the NP sequence between 20 and 8 MHz and PP sequence between 8 and 0.01 MHz. The observation field was set at 13 MHz. Sixteen experiments of two scans were used for the T_1 determination for each field. Water proton T_1 measurements at fixed frequency were carried out on a Stelar SpinMaster Spectrometer [Stelar S.n.c., Mede (PV), Italy] operating in the range from 20 to 80 MHz, by means of the inversion-recovery method (16 experiments, two scans). The reproducibility of the T_1 data was ±0.5%. All starting materials were obtained from Sigma-Aldrich Co. and were used without further purification. Gd–AAZTAC17 {AAZTAC17 = [6-bis(carboxymethyl)amino-4-carboxymethyl-6-heptadecyl-1, 4-diazepan-1-yl]acetic acid} was synthesized accordingly to the previously reported procedure (8). Adducts between Gd–AAZTAC17 and LDL were prepared following the already reported protocol (9). Briefly, Gd–AAZTAC17 was incubated with native human LDL (Biomedical Technology, Stoughton, MA, USA) at 37 °C for 2 h using a complex/LDL molar ratio of 300:1 and a Gd complex concentration lower than its cmc (0.08 mM). The LDL adducts were concentrated to a final volume of 1 ml using Vivaspin centrifuge filters (Sigma) (molecular weight cutoff = 10 000), and the unbound complex was eliminated by washing three times with 5 ml of PBS in the same tubes. The final Gd concentration was determined by ^{1}H NMR T_1 measurement of the mineralized complex solution (in 6 M HCl at 120 °C for 16 h) and the protein concentration was determined by a commercial Bradford assay (Biorad, Hercules, CA, USA).

The hydrated mean diameter of adducts was determined using a Malvern dynamic light-scattering spectrophotometer (Malvern Instruments, Malvern, UK). All samples were analyzed at 25 °C in filtered (cutoff = 30 nm) PBS buffer (pH 7).

4.1. Cell culture and uptake experiments

Mouse melanoma cell line (B16–F10) was obtained from the American Type Culture Corporation. The B16 were cultured in DMEM (Lonza) supplemented with 10% (v/v) FBS, 4 mM glutamine, 100 U ml^{-1} penicillin, and 100 µg ml^{-1} streptomycin. The cells were incubated at 37 °C in a humidified atmosphere of 5% CO_2. At 80% confluency, cells were trypsinized with 0.1% trypsin and 0.02% EDTA in PBS. For the *in vitro* uptake experiments, about 3×10^5 of B16 were seeded in 6 cm-diameter culture dishes. The day after, cells were incubated for 24 h with culture media added with 10% LPDS to increase LDLR expression. After 24 h, cells were incubated for 16 h with Gd–AAZTAC17/LDL adduct 60 µg ml^{-1} in protein. At the end of incubation, cells were washed three times with 10 ml ice-cold PBS, detached with trypsin–EDTA, and transferred into glass capillaries for MRI analysis (see below). Gd content of B16 was determined using inductively coupled plasma mass spectrometry (ICP-MS) (Element-2; Thermo-Finnigan, Rodano, Milan, Italy). Sample digestion was performed with 2 ml of concentrated HNO_3 (70%) under microwawe heating (Milestone MicroSYNTH Microwave labstation equipped with an optical fiber temperature control and HPR-1000/6 M six position high-pressure reactor, Bergamo, Italy). After digestion, sample volumes were brought to 2 ml with ultrapure water and samples were analyzed by ICP-MS. Protein concentration was determined from cell lysates by the Bradford method, using bovine serum albumin as standard.

4.2. Experimental mice and induction of transplantable tumors

Adult C57BL/6 mice were maintained in specific pathogen-free conditions at both the animal facilities of the Department of Genetica, Biologia e Biochimica, Molecular Biotechnology Center Turin University, Italy, and Charles River Laboratories (Calco, Italy). Handling and all manipulations were carried out in accordance with the European Community guidelines, and all the experiments were approved by the Ethical Committee of the

University of Turin. B16 cells line was cultured as described above and tumors were generated by subcutaneous injection into the right flank of 1×10^6 cells in 0.2 ml PBS. One week after B16 injection, mice developed solid tumors of 2–4 mm in diameter and were used for imaging evaluation.

4.3. MRI

All MR images were acquired th at the 7 T field on a Bruker Avance300 spectrometer equipped with a Micro 2.5 microimaging probe (Bruker BioSpin, Ettlingen, Germany) using two birdcage resonators with 30 and 10 mm inner diameter. MR images at 1 T were acquired with an Aspect M2-High Performance MRI System (Aspect Magnet Technologies Ltd, Netanya, Israel) consisting of a NdFeB magnet, equipped with a 35 mm solenoid Tx/Tr coil of inner diameter 35 mm. This system is equipped with fast gradient coils (gradient strength, 450 mT m^{-1} at 60 A; ramp time, 250 μs at 160 V) with a field homogeneity of 0.2–0.5 gauss.

For recording MR images *in vitro*, cells were dispersed at different densities (from 20 000 to 5000 cells μl^{-1}) in low gelling agarose gel (1% in PBS), and then transferred into glass capillaries. MR images were acquired using a standard T_1-weighted multislice spin echo sequence, using the following parameters: *TR*/*TE*/NEX 250/4/6, resolution 78 μm, slice thickness 1 mm at 7 T and *TR*/*TE*/NEX 250/7/16, resolution 78 μm, slice thickness 1 mm at 1 T, respectively. At both field strengths a standard saturation recovery protocol was used to measure T_1 relaxation times.

In vivo, before MRI examination, animals were anesthetized by injecting tiletamine–zolazepam (Zoletil 100; Virbac, Milan, Italy) 20 mg kg^{-1} + xylazine (Rompun; Bayer, Milan, Italy) 5 mg kg^{-1}. Gd–AAZTAC17/LDL (250:1) (0.06 mmol kg^{-1}) was injected through tail vein injection in three mice. MR images were acquired before, and 5 h after contrast administration using a standard T_1-weighted spin echo sequence, using the following parameters: at 7 T, *TR*/*TE*/NEX 250/4/6, resolution 234 μm, slice thickness 1 mm; at 1 T, *TR*/*TE*/NEX 250/7/16, resolution 273 μm, slice thickness 1 mm.

The mean signal intensity (SI_0) values were calculated on a region of interest (ROI) manually drawn on the whole tumor. The measured SI was normalized to a standard Gd(III) solution to take into account differences in the absolute signal intensity values among different images obtained after mouse repositioning in the MRI scanners. The normalization was carried out by dividing the SI_0 values of the ROI drawn on the tumor to the SI values of the ROI drawn inside the reference tube (SI_{ref}).

$$\text{SI normalized}\,(SI_n) = SI_0/SI_{ref}$$

The mean SI enhancement (percentage enhancement) of target tissues (TT) was calculated according to the following equation:

$$\text{SI \% enhancement} = [(\text{mean } SI_n(\text{TT}) \text{ post contrast} - \text{mean } SI_n(\text{TT}) \text{ pre} - \text{contrast}]/\text{mean } SI_n(\text{TT}) \text{ pre} - \text{contrast}) \times 100$$

SNR and CNR have been calculated as follows:

$$\text{SNR} = SI_{mus}/\sigma_n$$

where SI_{mus} is the signal intensity measured on a ROI outlined on a muscle region and σ_n is the standard deviation of a ROI drawn in the air outside the animal.

$$\text{CNR} = (SI_{tum} - SI_{mus})/\sigma_n$$

where SI_{tum} and SI_{mus} are SI of tumour and muscle, respectively.

Acknowledgments

This work was supported by Regione Piemonte Nano-IGT project (Converging Technologies), ENCITE-project (FP7-HEALTH-2007-A), Meditrans (NMP4-CT-2006-026668) and EU Action COST D38.

REFERENCES

1. Rinck PA. Magnetic Resonance in Medicine. Blackwell Scientific: Oxford, 2003.
2. Merbach AE, Toth E. The Chemistry of Contrast Agents in Medical Magnetic Resonance Imaging. John Wiley & Sons, Chichester, 2001.
3. Geraldes CFGC, Laurent S. Classification and basic properties of contrast agents for magnetic resonance imaging. Contrast Media Mol Imag 2009; 4: 1–23.
4. Aime S, Delli Castelli D, Geninatti Crich S, Gianolio E, Terreno E. Pushing the sensitivity envelope of lanthanide-based magnetic resonance imaging (MRI) contrast agents for molecular imaging applications. Acc Chem Res 2009; 42: 822–831.
5. Lauffer RB. Paramagnetic metal complexes as water proton relaxation agents for NMR imaging: theory and design. Chem Rev 1987; 87: 901–927.
6. Aime S, Geninatti-Crich S, Gianolio E, Giovenzana GB, Tei L, Terreno E. High sensitivity lanthanide(III) based probes for MR-medical imaging. Coord Chem Rev 2006; 1562–1579.
7. Caravan P. Protein-targeted gadolinium-based magnetic resonance imaging (MRI) contrast agents: design and mechanism of action. Acc Chem Res 2009; 42: 851–862.
8. Gianolio E, Giovenzana GB, Longo D, Longo I, Menegotto I, Aime S. Relaxometric and modelling studies of the binding of a lipophilic Gd–AAZTA complex to fatted and defatted human serum albumin. Chemistry 2007; 13(20): 5785–5797.
9. Geninatti-Crich S, Lanzardo S, Alberti D, Belfiore S, Ciampa A, Giovenzana GB, Lovazzano C, Pagliarin R, Aime S. Magnetic resonance imaging detection of tumor cells by targeting low-density lipoprotein receptors with Gd-loaded low-density lipoprotein particles. Neoplasia 2007; 9(12): 1046–1056.
10. Firestone RA. Low density lipoprotein as a vehicle for targeting antitumor compounds to cancer cells. Bioconjug Chem 1994; 5: 105–113.
11. Versluis AJ, van Geel PJ, Oppelaar H, van Berkel TJ, Bijsterbosch MK. Receptor-mediated uptake of low-density lipoprotein by B16 melanoma cells in vitro and in vivo in mice. Br J Cancer 1996; 74: 525–532.
12. Glickson JD, Lund-Katz S, Zhou R, Choi H, Chen IW, Li H, Corbin I, Popov AV, Cao W, Song L, Qi C, Marotta D, Nelson DS, Chen J, Chance B, Zheng G. Lipoprotein nanoplatform for targeted delivery of diagnostic and therapeutic agents. Adv Exp Med Biol 2009; 645: 227–239.
13. Brown MS, and Goldstein JL. Receptor-mediated endocytosis: insights from the lipoprotein receptor system. Proc Natl Acad Sci USA 1979; 76(7): 3330–3337.
14. Goldstein JL, Brown MS. The LDL receptor. Arterioscler Thromb Vasc Biol 2009; 29(4): 431–438.
15. Terreno E, Geninatti Crich S, Belfiore S, Biancone L, Cabella C, Esposito G, Manazza AD, Aime S. Effect of the intracellular localization of a Gd-based imaging probe on the relaxation enhancement of water protons. Magn Reson Med 2006; 55(3): 491–497.
16. Geninatti Crich S, Cabella C, Barge A, Belfiore S, Ghirelli C, Lattuada L, Lanzardo S, Mortillaro A, Tei L, Visigalli M, Forni G, Aime S. In vitro and in vivo magnetic resonance detection of tumor cells by targeting glutamine transporters with Gd-based probes. J Med Chem 2006; 49(16): 4926–4936.
17. Strijkers GJ, Hak S, Kok MB, Springer CS Jr, Nicolay K. Three-compartment T_1 relaxation model for intracellular paramagnetic contrast agents. Magn Reson Med 2009; 61(5): 1049–1058.

